Small-Signal Stability Criterion for Inertial and Primary Frequency Droop Control of MTDC Grids Connected to Asynchronous AC Systems

Sai Gopal Vennelaganti[1] and Nilanjan Ray Chaudhuri[2]

***Abstract*— Droop control strategy is widely used for exchanging frequency support amongst asynchronous AC areas through multiterminal DC (MTDC) grid. We provide analytical constraints on inertial and primary frequency droop coefficients as sufficient conditions of small-signal stability when both of the droop controls are active. To this end, a reduced-order model of the system is presented followed by salient observations leading up to the formulation of a stability theorem. The theorem is proved based on two lemmas, where the first lemma derives the sufficient condition for ensuring negative real parts of the eigenvalues of a matrix using the continuity argument of its eigenvalues with respect to its elements. The second lemma expresses the system matrix as rank-1 perturbation of a diagonal matrix, which greatly simplifies the proof. Finally, the analytical stability region in droop coefficient space is compared with the numerically-obtained stability region from the full-order model of an example test system.**

I. Introduction

The August 2019 UK blackout due to underfrequency load shedding [1] has highlighted the need for frequency support among asynchronous AC systems since each of such areas are experiencing depleting inertia. We believe that the existing HVDC cross-channel link between UK and France could have been used for this purpose and avert the blackout. In view of the envisioned Super Grid project, which aims to connect various asynchronous AC areas in Europe and Africa [2], there is a need to synthetically provide frequency support through the interconnecting Multiterminal High Voltage Direct Current (MTDC) grid. Literature on frequency support can be broadly divided into two groups (i) distributed/coordinated/centralized methods [3]–[9] and (ii) droop control-based methods.

Consensus-based control strategies are proposed in references [3] and [4]. Multiple papers [5], [6] build on this concept to propose different distributed controllers in the forms of model predictive control (MPC) and proportional-integral (PI) control. Such distributed controllers have also been proposed for automatic generation control (AGC) [7], [8]. Notably, in all these works [3]–[8] small-signal stability is analytically proved at least for some special cases. On the other hand, [9] proposed MPC for secondary frequency control, where parameter design is based on trial and error approach.

Reference [10] is the first paper to employ droop control to provide frequency support through MTDC grid, following which multiple works on this topic have used droop in some form. Reference [11] is first to present a communication-free droop control to extract support from offshore wind farms (OWFs). Related works on frequency support from OWFs include [12] and [13]. A few papers [14], [15] analyze the effect of coupling between voltage and frequency droop in steady state. To decouple the droop control loops, [16] proposes an integration method, [17], [18] presents a receding horizon control, and [19] proposed a MPC-based approach. Some works on adaptive frequency support include [20], [21]. Reference [20] proposes emulation of a virtual synchronous generator through voltage source converter (VSC) controls to extract inertial and primary frequency support. In [21], voltage-droop coefficients are adaptively varied based on the frequency deviation.

To the best of our knowledge, none of the papers, [3]–[21] consider any aspects of stability with regards to choice of droop coefficients. Our prior works [22], [23] propose a ratio-based approach to quantify the support provided by a single AC area towards the interconnection. In those works, the droop coefficients are analytically designed to meet the prescribed ratios based on a reduced Nth-order model. Reference [24] achieves the objective of ratio-based frequency support by explicitly communicating the system frequencies that neglects communication delay. However, [22]–[24] does not establish any sufficient condition for system stability – only numerical root locus analysis is presented.

Notably, [22], [23] demonstrates feasibility of ratio-based control in presence of both inertial and primary frequency droop mechanisms working *simultaneously*. However, in our previous work [25], we are able to present sufficient conditions of small-signal stability only for two special cases where *either* of inertial or primary frequency droop coefficients are active. *The goal of this paper is to fill this gap by presenting a complete analytical proof of small-signal stability with inertial and primary frequency support acting together.*

The paper is organized as follows. For the sake of completeness, first a reduced Nth-order model of the asynchronous AC systems connected by MTDC grids is presented. Next, a summary of observations are presented that leads to the formulation of our stability theorem. Finally, we present a couple of important lemmas and build on them to prove the proposed theorem. We evaluate the conservatism of the proposed theorem by comparing the region of stability in the droop coefficient space in the Nth-order model with numerically calculated stability region from a detailed phasor-based differential-algebraic representation of the AC-

Financial support from NSF Grant Award ECCS 1656983 is gratefully acknowledged. [1]Sai Gopal Vennelaganti is with Tesla, Inc. [2]Nilanjan Ray Chaudhuri is with The School of Electrical Engineering & Computer Science, The Pennsylvania State University, University Park, PA 16802, USA. sps6260@psu.edu, nuc88@psu.edu

(a) Generic N-Asynchornous AC Area System:

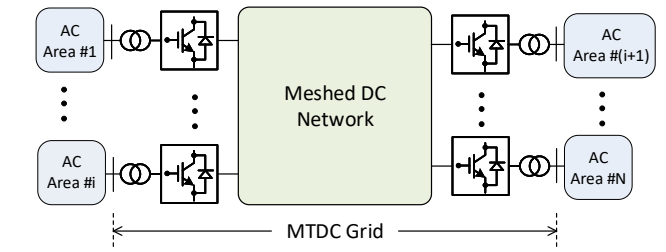

(b) Inertial and Frequency Droop Controller in Area #i:

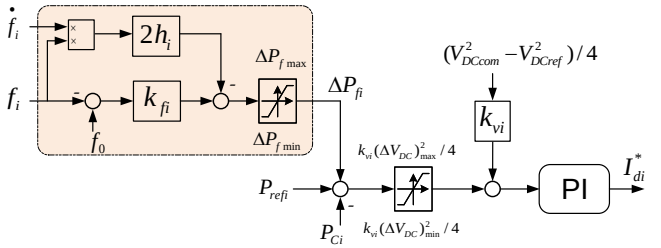

Fig. 1: Representation of the power-frequency-inertial-voltage droop controller in ith AC area.

MTDC grid, i.e., the full-order model.

II. Review: Nth-order Model of N-Asynchronous AC Area System Connected to MTDC Grid

For the sake of completeness, we review the reduced Nth-order model of the MTDC grid connected to N asynchronous AC areas shown in Fig. 1(a). The objective is to adequately represent the *averaged* frequency dynamics of this system. To that end, we neglect losses in the AC and DC systems and only retain the swing dynamics of synchronous generators in an aggregated form for each AC area, where H_G, k_{gov} and P_M are the equivalent inertia constant, aggregated governor droop coefficient, and aggregated mechanical power input to synchronous generators, respectively, and P_L is the aggregated load.

The outer loop of converter controller with inertial and primary frequency droop control in the ith AC area is shown in Fig. 1(b). The parameters k_{fi}, h_i, and k_{vi} represent the primary frequency, inertial, and DC voltage droop coefficients, respectively. From now on, we will use 'frequency droop' to imply 'primary frequency droop.' Assuming ideal tracking performance of the PI controller, we can write

$$\begin{aligned} P_{Ci} = P_{refi} + k_{fi}\Delta f_i - 2h_i f_i \dot{f}_i \\ + k_{vi}(V^2_{DCcom} - V^2_{DCref})/4 \end{aligned} \tag{1}$$

where, subscripts i and ref denote the ith AC area and reference quantity, respectively; P_C is the net power injected into the AC area from the MTDC grid; V_{DCcom} is the dc-link voltage communicated from the so-called pilot bus [26] through the fiber optic cable embedded in the power cable; f is frequency and $\Delta f_i = f_0 - f_i$ is the frequency deviation from the nominal value f_0.

The swing equation of the aggregated synchronous generator in the ith ac area can be written as

$$2H_{Gi} f_i \dot{f}_i = P_{Mi} + k_{govi}\Delta f_i - P_{Li} + P_{Ci} \tag{2}$$

After replacing P_{Ci} from (1) in (2) and following some algebraic manipulations, the equations governing the frequency dynamics of the reduced model can be written as,

$$\begin{aligned} &2[H_{Gi} + (1-\bar{k}_{vi})h_i] f_0 \dot{f}_i - \bar{k}_{vi}\Big(\sum_{k\neq i}^{N} 2h_k f_0 \dot{f}_k\Big) \\ &= [k_{govi} + (1-\bar{k}_{vi})k_{fi}]\Delta f_i - \bar{k}_{vi}\Big(\sum_{k\neq i}^{N} k_{fk}\Delta f_k\Big) + \Delta P_i \end{aligned} \tag{3}$$

where, $i = 1,\ldots,N$; $\bar{k}_{vi} = k_{vi}/\sum_k^N k_{vk}$ is the normalized voltage-droop coefficient, and ΔP_i is given by,

$$\Delta P_i = P_{Mi} - P_{Li} + P_{refi} - \bar{k}_{vi}\Big(\sum_{k}^{N} P_{refk}\Big) \tag{4}$$

From (3), the Nth-order model can be represented by the following equation, (note that $\Delta f_i = f_0 - f_i$ implies, $\dot{f}_i = -\Delta\dot{f}_i$)

$$2f_0 \mathbf{H_N} \Delta\dot{\mathbf{f}} = -\mathbf{K_N}\Delta\mathbf{f} - \Delta\mathbf{P} \tag{5}$$

Here, the i^{th} elements of vectors $\Delta\mathbf{P} \in \mathbb{R}^N$ and $\Delta\mathbf{f} \in \mathbb{R}^{\mathbf{N}}$ are ΔP_i and Δf_i, respectively. Note that $\Delta\mathbf{P}$ is an input to the system model (5) representing ac and/or dc-side disturbances in the system, which is equal to $\mathbf{0}$ under steady state. The matrices $\mathbf{H_N} \in \mathbb{R}^{N\times N}$ and $\mathbf{K_N} \in \mathbb{R}^{N\times N}$ have similar structures and their elements are given by,

$$\begin{aligned} H_N(i,j) &= \begin{cases} H_{Gi} + (1-\bar{k}_{vi})h_i & \text{if } i = j \\ -\bar{k}_{vi}h_j & \text{if } i \neq j \end{cases} \\ K_N(i,j) &= \begin{cases} k_{govi} + (1-\bar{k}_{vi})k_{fi} & \text{if } i = j \\ -\bar{k}_{vi}k_{fj} & \text{if } i \neq j \end{cases} \end{aligned} \tag{6}$$

Note that such a structure stems from the pilot bus-based droop control mentioned earlier. In case of a local dc-link voltage based droop control, with the approximation of negligible dc voltage drops in lines, a similar structure might be obtained. The condition for (global) exponential stability of (5) is,

$$\big\{\Re(\lambda_i((\mathbf{H_N})^{-1}\mathbf{K_N})),\ i = 1,\ldots,N\big\} \subset \mathbb{R}_{>0} \tag{7}$$

where, $\Re(\lambda_i(\cdot))$ is the real part of the ith eigenvalue of a square matrix and $\mathbb{R}_{>0}$ denotes the set of positive real numbers. In a compact form, we represent the condition in (7) as $\Re(\lambda((\mathbf{H_N})^{-1}\mathbf{K_N})) \succ \mathbf{0}$.

III. Region of Stability in Droop Coefficient Space

Clearly, the choice of droop coefficients (h_i and k_{fi}) affects the stability of the Nth order model (5). Our goal is to establish a region of stability in the droop coefficient space, which can be very helpful in control design. To that end a Stability Hypothesis was proposed in [25], which was proved for two special cases where **either** of frequency droop (Mode I) **or** inertial droop (Mode

II) are active that satisfy $\Re(\lambda((\mathbf{H_N}|_{h_i=0:\forall i})^{-1}\mathbf{K_N})) \succ \mathbf{0}$ or $\Re(\lambda((\mathbf{K_N}|_{k_{fi}=0:\forall i})^{-1}\mathbf{H_N})) \succ \mathbf{0}$, respectively. In this paper, we present the proof for the general case where **both** inertial and frequency droop coefficients are active (Mode III). With this proof, we change the 'Hypothesis' to a 'Theorem.' Next, the observations leading up to the formulation of the stability theorem are described.

A. Observations Towards Formulating Stability Theorem [25]

We make salient observations relating the eigenvalues of the system operating under Mode I or (equivalently) Mode II. Although these are special cases of Mode III, they help us formulate the stability theorem. For convenience of notation, we express the system matrix under these modes as in (8), where $\hat{\mathbf{H}}_\mathbf{N} = (\mathbf{K_N}|_{k_{fi}=0:\forall i})^{-1}\mathbf{H_N}$ and $\hat{\mathbf{K}}_\mathbf{N} = (\mathbf{H_N}|_{h_i=0:\forall i})^{-1}\mathbf{K_N}$. Now we consider certain points in the droop coefficient space and evaluate the eigenvalues of $\hat{\mathbf{X}}_\mathbf{N}$.

1) Observation-I: For $x_i = -C_i \ \forall \ i$, we find that $\hat{\mathbf{X}}_\mathbf{N}$ has all zero eigenvalues except one positive real eigenvalue. In this case, the system is marginally stable and not in block-Jordan form, because all the eigenvectors with zero eigenvalues are independent vectors.

2) Observation-II: Let, $x_i = -C_i + pD_i \ \forall \ i$, where $p > 0$ is some positive real constant. We see that all eigenvalues are positive real, out of which $N-1$ are equal to p. Hence, the system is stable for this set of droop coefficients.

3) Observation-III: Considering $x_1 = x_{10} > -C_i$ and $x_i = -C_i \ \forall \ i \neq 1$, we find that there are all but two non-zero eigenvalues that are either positive when real or have a positive real part when they are a complex conjugate pair leading to a marginally stable system.

4) Observation-IV: Finally, using $x_1 = x_{10} + pD_1$ and $x_i = -C_i + pD_i \ \forall \ i \neq 1$, where $x_{10} > -C_1$ and $p > 0$ is some positive real constant, we obtain $N-2$ positive-real eigenvalues of value p, while the remaining two eigenvalues have positive real parts leading to a stable system.

In summary, within a coordinate system in the droop coefficient space with origin at $x_i = -C_i \ \forall \ i$ and the unit vectors $\hat{e}_i$s as the basis vectors,

1) The origin of the coordinate system and points along any positive axis lead to We formulate the stability theorem based on the a marginally stable system.
2) Starting from any of the above-stated marginally stable points, moving in the direction of vector $[D_1, \cdots, D_N]^T$ into the positive quadrant of the constructed coordinate system makes the system stable.

We formulate the stability theorem based on the foregoing observations.

Theorem III.1. *The N^{th}-order system is small-signal stable, i.e., constraint* (7) *will be met if inertial and frequency droop coefficients satisfy $h_i > -H_{Gi}$ and $k_{fi} > -k_{govi}$.*

In this paper, we approach the problem of handling $(\mathbf{H_N})^{-1}$ in (7) by first expressing $\mathbf{H_N}$ as the rank-1 perturbation of a diagonal matrix and then apply Sherman-Morrison formula [27]. This helps us apply Lemma I in [25] on $(\mathbf{H_N})^{-1}\mathbf{K_N}$, which in turn leads to the proof of this theorem. The validity of the proposed conditions are verified using eigenvalue analysis of the full-order model.

B. Formal Proof of Stability Theorem

To prove the stability for Modes I and II, we proposed a lemma in [25] that is based on continuity argument of eigenvalues of a matrix with respect to its parameters. We will need this lemma to prove Theorem III.1 as well. Therefore, we include the lemma and its proof here for sake of completeness.

Lemma III.2. *Given a matrix, $\mathbf{M}(\tau)$ such that, all its elements are continuous functions of parameter $\tau \in \mathbb{R}^n$ $\big($i.e, $\mathbf{M}(\tau) = [m_{ij}(\tau)]$, where m_{ij} is continuous w.r.t. $\tau \ \forall \ i, j\big)$, then $\Re(\lambda(\mathbf{M}(\tau))) \prec \mathbf{0} \ \forall \ \tau \in \mathcal{S} \subseteq \mathbb{R}^n$,if the region $\mathcal{S}$ satisfies the following conditions,*

1) *$\mathcal{S}$ is connected,*
2) *$\exists$ at least one $\tau^* \in \mathcal{S}$ s.t. $\Re(\lambda(\mathbf{M}(\tau^*))) \prec \mathbf{0}$,and*
3) *$\nexists \ \tau \in \mathcal{S}$, s.t. at least one eigenvalue of $\mathbf{M}(\tau)$ has real part zero.*

Remark: In [28] it is established that zeros of a polynomial are continuous with respect to its coefficients, which implies that eigenvalues of a matrix are continuous with respect to its elements. Consequently, the eigenvalues, specifically the real part of the eigenvalues of the matrix $\mathbf{M}(\tau)$ are continuous w.r.t. τ. This fact has been used in many robust stability proofs of [29]. ■

Proof: For the sake of contradiction, assume that $\exists \ \bar{\tau} \in \mathcal{S}$ such that at least one eigenvalue of $\mathbf{M}(\bar{\tau})$ has a positive real part. From condition (2), $\exists \ \tau^* \in \mathcal{S}$ such that $\Re(\lambda(\mathbf{M}(\tau^*))) \prec \mathbf{0}$.Since $\tau^*, \bar{\tau} \in \mathcal{S}$, which is a connected region in $\mathbb{R}^n$, we can construct a path, $\mathcal{P}$ between τ^* and $\bar{\tau}$ such that $\mathcal{P} \subseteq \mathcal{S}$. Figure 2 illustrates the path $\mathcal{P}$ in $\mathcal{S}$. The real part of the eigenvalues should continuously change as we vary τ along the path, $\mathcal{P}$ from τ^* to $\bar{\tau}$. This implies that $\exists \ \tau^0 \in \mathcal{P} \subseteq \mathcal{S}$ as shown in Fig. 2 such that at least one eigenvalue of $\mathbf{M}(\boldsymbol{\tau^0})$ has real part zero. However, this contradicts condition (3). Hence, by contradiction we have $\Re(\lambda(\mathbf{M}(\tau))) \prec \mathbf{0} \ \forall \ \tau \in \mathcal{S}$. ■

From equation (5), it is clear that the system matrix of this reduced linear system is $-\mathbf{H_N}^{-1}\mathbf{K_N}/(2f_0)$. Looking at the form of the matrices from (6), it appears a bit challenging to derive constraints on h_is and k_{fi}s that satisfy (7). To achieve this, we present the following lemma.

Lemma III.3. *The matrix $\mathbf{G} = -(\mathbf{H_N})^{-1}\mathbf{K_N}/(2f_0)$ can be expressed as the rank-1 perturbation of a diagonal matrix.*

Proof: Note that the matrix $\mathbf{H_N}$, can be expressed as the sum of a diagonal matrix and a rank-1 matrix as follows,

$$\mathbf{H_N} = diag([(h_i + H_{Gi})]_N) - \left[\bar{k}_{vi}\right]_N \left[h_i\right]_N^T \tag{9}$$

Here, $[a_i]_N := [a_1 \cdots a_N]^T$. Recognizing that this is of the form, $\mathbf{A} + \mathbf{uv^T}$, the inverse of this matrix $\mathbf{H_N}^{-1}$ can be

$$\hat{\mathbf{X}}_\mathbf{N} = \begin{bmatrix} [C_1+(1-\bar{k}_{v1})x_1]/D_1 & -\bar{k}_{v1}x_2/D_1 & \cdots & -\bar{k}_{v1}x_N/D_1 \\ -\bar{k}_{v2}x_1/D_2 & [C_2+(1-\bar{k}_{v2})x_2]/D_2 & \cdots & -\bar{k}_{v2}x_N/D_2 \\ \vdots & \vdots & \ddots & \vdots \\ -\bar{k}_{vN}x_1/D_N & -\bar{k}_{vN}x_2/D_N & \cdots & [C_N+(1-\bar{k}_{vN})x_N]/D_N \end{bmatrix} = \begin{cases} \hat{\mathbf{H}}_\mathbf{N} & \text{if, } (x_i,C_i,D_i) \\ & = (h_i,H_{Gi},k_{govi}) \\ \hline \hat{\mathbf{K}}_\mathbf{N} & \text{if, } (x_i,C_i,D_i) \\ & = (k_{fi},k_{govi},H_{Gi}) \end{cases} \tag{8}$$

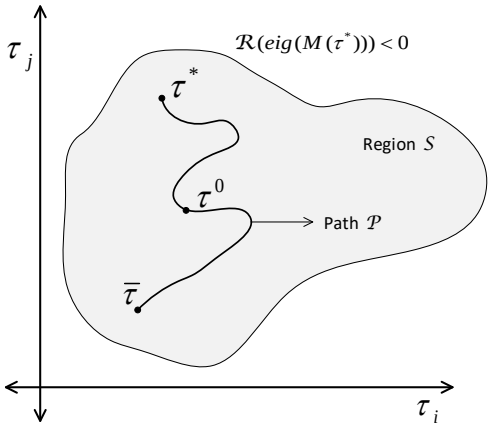

Fig. 2: Illustration of proof of Lemma-I.

derived using the Sherman-Morrison formula [27],

$$(\mathbf{A}+\mathbf{u}\mathbf{v}^\mathbf{T})^{-1} = \mathbf{A}^{-1} - \frac{\mathbf{A}^{-1}\mathbf{u}\mathbf{v}^\mathbf{T}\mathbf{A}^{-1}}{1+\mathbf{v}^\mathbf{T}\mathbf{A}^{-1}\mathbf{u}} \tag{10}$$

Since the $\mathbf{A}$ in equation (9) is diagonal, through simplifications, the inverse of $\mathbf{H_N}$ can be derived as follows,

$$\begin{aligned}(\mathbf{H_N})^{-1} &= diag([1/(h_i+H_{Gi})]_N) \\ &\quad + \left[\bar{k}_{vi}/(h_i+H_{Gi})\right]_N \left[h_i/(h_i+H_{Gi})\right]_N^T/w\end{aligned} \tag{11}$$

where, w is given by $\sum_{i=1}^N \frac{\bar{k}_{vi}H_{Gi}}{(h_i+H_{Gi})}$. Multiplying this with $\mathbf{K_N}$, we can derive the system matrix as follows (see, Appendix),

$$\begin{aligned}\mathbf{G} &= -(\mathbf{H_N})^{-1}\mathbf{K_N}/(2f_0) \\ &= -\frac{1}{2f_0}diag\left(\left[\frac{k_{fi}+k_{govi}}{h_i+H_{Gi}}\right]_N\right) \\ &\quad -\frac{1}{2f_0 w}\left[\frac{\bar{k}_{vi}}{h_i+H_{Gi}}\right]_N\left[\frac{k_{govi}h_i - H_{Gi}k_{fi}}{h_i+H_{Gi}}\right]_N^T\end{aligned} \tag{12}$$

Hence proved. ■

Proof of Theorem III.1: We note that constraint (7) is equivalent to $\Re(\lambda(\mathbf{G})) \prec \mathbf{0}$.Let us say τ_x is formed by concatenation of h_is and k_{fi}s, i.e., $\tau_x = [h_1 \cdots h_N, k_{f1} \cdots k_{fN}]^T$. From (12), we can see that the elements of matrix $\mathbf{G}$ are continuous functions of τ_x.

Let $\mathcal{S}_x \triangleq \{\tau_x \mid h_i > -H_{Gi}, k_{fi} > -k_{govi}\ \forall\ i \le N\}$. In order to prove that $\Re(\lambda(\mathbf{G})) \prec \mathbf{0}\ \forall\ \tau_x \in \mathcal{S}_x \subseteq \mathbb{R}^{2N}$, Lemma-I can be used if region $\mathcal{S}_x$ satisfies the three above-stated conditions.

(1) By definition, we know that the region $\mathcal{S}_x$ is connected.

(2) For satisfying the second condition, we use the result of Lemma III.3. By setting $\tau_x = 0$, i.e., $h_i = 0,\ k_{fi} = 0\ \forall i$, the matrix $\mathbf{G}$ in (12) will be simplified into a diagonal matrix $-\frac{1}{2f_0}diag\left(\left[\frac{k_{govi}}{H_{Gi}}\right]_N\right)$. Since $k_{govi} > 0,\ H_{Gi} > 0\ \forall i$, it satisfies $\Re(\lambda(\mathbf{G})) \prec \mathbf{0}$.

(3) We prove condition (3) by contradiction – we assume that $\exists\ \mathbf{v} \in \mathbb{R}^N$, s.t. $\mathbf{G}\mathbf{v} = \sqrt{-1}\lambda_{im}\mathbf{v}$ for some $\lambda_{im} \in \mathbb{R}$ and $\forall\ \tau_x \in \mathcal{S}_x$, then we show that $\mathbf{v}$ has to be $\mathbf{0}$.

For simplification, let $c_i := H_{Gi}$, $d_i := k_{govi}$, $p_i := h_i + H_{Gi}$, $q_i := k_{fi} + k_{govi}$ and $\bar{\mathbf{G}} := -2f_0\mathbf{G}$. With this, we have, $c_i, d_i, p_i, d_i > 0$. Again, using result from Lemma III.3 we get,

$$\bar{\mathbf{G}} = diag\left(\left[\frac{q_i}{p_i}\right]_N\right) + \frac{1}{w}\left[\frac{\bar{k}_{vi}}{p_i}\right]_N\left[\frac{d_ip_i - c_iq_i}{p_i}\right]_N^T \tag{13}$$

Now we assume that for the matrix $\bar{\mathbf{G}}$ $\exists$ a eigenvector $\mathbf{v} = \left[a_i + \sqrt{-1}b_i\right]_N$ with a corresponding eigenvalue of '$\sqrt{-1}\lambda$', i.e., on the imaginary axis, where $\lambda \in \mathbb{R}$. From linear algebra we know that $\bar{\mathbf{G}}\mathbf{v} = \sqrt{-1}\lambda\mathbf{v}$, this implies,

$$\begin{aligned}&\left(diag\left(\left[\frac{q_i}{p_i}\right]_N\right) + \frac{1}{w}\left[\frac{\bar{k}_{vi}}{p_i}\right]_N\left[\frac{d_ip_i - c_iq_i}{p_i}\right]_N^T\right)\left[a_i+\sqrt{-1}b_i\right]_N \\ &\qquad = \sqrt{-1}\lambda\left[a_i+\sqrt{-1}b_i\right]_N\end{aligned} \tag{14}$$

Upon multiplying and equating the real and imaginary parts from either side of ith row of (14), we have,

$$\begin{aligned}a_iq_i + \frac{\lambda b_ip_i}{w} &= \frac{\bar{k}_{vi}}{w}\sum_j a_j\left(\frac{c_jq_j}{p_j} - d_j\right) \\ b_iq_i - \frac{\lambda a_ip_i}{w} &= \frac{\bar{k}_{vi}}{w}\sum_j b_j\left(\frac{c_jq_j}{p_j} - d_j\right)\end{aligned} \tag{15}$$

The summation terms on the right hand side are same for every i. Let $A := \sum_j a_j\left(\frac{c_jq_j}{p_j} - d_j\right)$ and $B := \sum_j b_j\left(\frac{c_jq_j}{p_j}d_j\right)$. We can write (15) in a matrix form as shown below,

$$\begin{bmatrix} q_i & \frac{\lambda p_i}{w} \\ -\frac{\lambda p_i}{w} & q_i \end{bmatrix}\begin{bmatrix} a_i \\ b_i \end{bmatrix} = \frac{\bar{k}_{vi}}{w}\begin{bmatrix} A \\ B \end{bmatrix} \tag{16}$$

Through some algebraic manipulations, we shall prove that A and B have no choice but to be zero. Since, the matrix on the right hand side is full-rank (determinant is $q_i^2 + \frac{\lambda^2 p_i^2}{w^2} > 0$), it can be inverted, by extension, a_i and b_i have to be zero.

Summing up and subtracting both rows in the (16), we get,

$$\begin{aligned}(a_i+b_i)q_i + \frac{\lambda p_i}{w}(b_i-a_i) &= \frac{\bar{k}_{vi}}{w}(A+B) \\ (a_i-b_i)q_i + \frac{\lambda p_i}{w}(a_i+b_i) &= \frac{\bar{k}_{vi}}{w}(A-B)\end{aligned} \tag{17}$$

In order to eliminate q_i, we rearrange (17) and multiply either side with c_i/p_i,

$$\begin{aligned}(a_i+b_i)\frac{c_iq_i}{p_i} &= \frac{c_i}{w}\left[\frac{\bar{k}_{vi}}{p_i}(A+B) - \lambda(b_i-a_i)\right] \\ (a_i-b_i)\frac{c_iq_i}{p_i} &= \frac{c_i}{w}\left[\frac{\bar{k}_{vi}}{p_i}(A-B) - \lambda(a_i+b_i)\right]\end{aligned} \tag{18}$$

From the definition of A and B, we know that,

$$\begin{aligned} A+B &= \sum_j \left(\frac{c_j q_j}{p_j}(a_j+b_j)\right) - \sum_j d_j(a_j+b_j) \\ A-B &= \sum_j \left(\frac{c_j q_j}{p_j}(a_j-b_j)\right) - \sum_j d_j(a_j-b_j) \end{aligned} \tag{19}$$

In the above equations, replacing the terms that has q_i with those in (18), we get,

$$\begin{aligned} A+B &= \frac{A+B}{w}\sum_j \left(\frac{c_j \bar{k}_{vj}}{p_j}\right) + \sum_j \frac{c_j}{w}(a_j-b_j) - \sum_j d_j(a_j+b_j) \\ A-B &= \frac{A-B}{w}\sum_j \left(\frac{c_j \bar{k}_{vj}}{p_j}\right) - \sum_j \frac{c_j}{w}(a_j+b_j) - \sum_j d_j(a_j-b_j) \end{aligned} \tag{20}$$

Since, A, B and w are independent of j, they can be taken out of summation. Recalling that, by definition $w = \sum_j \left(\frac{c_j \bar{k}_{vj}}{p_j}\right)$. Therefore, A and B can be eliminated,

$$\begin{aligned} \sum_j d_j(a_j+b_j) - \sum_j \frac{c_j}{w}(a_j-b_j) &= 0 \\ \sum_j d_j(a_j-b_j) + \sum_j \frac{c_j}{w}(a_j+b_j) &= 0 \end{aligned} \tag{21}$$

From (16), we can express a_i and b_i in terms of A and B by inverting the matrix as follows,

$$a_i = \frac{\bar{k}_{vi}(q_i w A - p_i \lambda B)}{q_i^2 w^2 + p_i^2 \lambda^2} \;;\; b_i = \frac{\bar{k}_{vi}(p_i \lambda A + q_i w B)}{q_i^2 w^2 + p_i^2 \lambda^2} \tag{22}$$

Substituting, the above expression for a_i and b_i in (21) and rearranging terms we finally get the following matrix,

$$\begin{bmatrix} s & t \\ -t & s \end{bmatrix} \begin{bmatrix} A \\ B \end{bmatrix} = \begin{bmatrix} 0 \\ 0 \end{bmatrix} \tag{23}$$

where, s and t are given by,

$$s = \sum_j \frac{\bar{k}_{vj}\left(w q_j d_j + \frac{\lambda^2}{w} p_j c_j\right)}{q_j^2 w^2 + p_j^2 \lambda^2} > 0 \;\;;\;\; t = \sum_j \frac{\bar{k}_{vj}\left(p_j d_j q_j c_j\right)\lambda}{q_j^2 w^2 + p_j^2 \lambda^2} \tag{24}$$

This implies that $A, B, a_i, b_i = 0 \forall i$ and that if there were to be an eigenvalue $\sqrt{-1}\lambda$, on the imaginary axis, satisfying $\bar{\mathbf{G}}\mathbf{v} = \sqrt{-1}\lambda\mathbf{v}$, the vector $\mathbf{v}$, has to be $\mathbf{0}$, and it contradicts the definition of the eigenvector. Therefore, there does not exist any eigenvalues on the imaginary axis. Hence proved.

Therefore, $\forall\ \tau_x \in \mathcal{S}_x$, we have $\Re(\lambda(\mathbf{G})) \prec \mathbf{0}$. ■

IV. Case Studies

We consider a test system where a 5-terminal MTDC grid is connected to 4 asynchronous AC grids as shown in Fig. 3. The following details are considered in this model [30] –

1) An averaged model of the converters with standard vector control scheme have been included.
2) Positive and negative poles along with metallic return network has been assumed, each of which are modeled using π-section dynamic models.
3) The AC transmission systems are modeled algebraically, whereas constant impedance load models are considered.

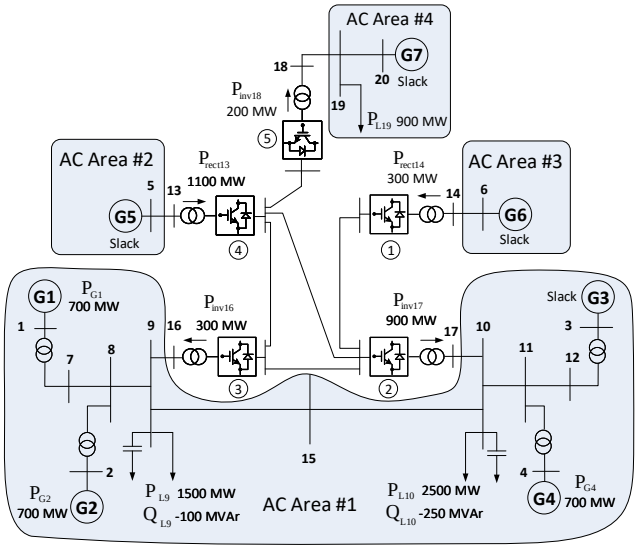

Fig. 3: Schematic of the bipolar MTDC grid with metallic return (single-line diagram) connecting 4 asynchronous AC areas.

4) The synchronous generators are represented by detailed sixth-order subtransient models with DC-1A exciters.

It is assumed that AC area-3 is not participating in frequency support. In other words, we consider the droop coefficient space with variables $\tau_x = [h_1, h_2, h_4, k_{f1}, k_{f2}, k_{f4}]^T$, where the subscripts denote the AC area #. For example, h_1 is the sum of inertial droop coefficients in converter stations 2 and 3 in Fig. 3. The inverse governor droop coefficients of the participating areas are $(k_{gov1},\ k_{gov2},\ k_{gov4}) = (212.20,\ 53.05,\ 53.05)\ MW/Hz$ and the effective inertia constants of the corresponding areas are $(H_{G1},\ H_{G2},\ H_{G4}) = (228.15,\ 185.25,\ 74.10)\ s^{-1}$ on 100 MVA base. Going forward, the frequency droop coefficients and the inertial droop coefficients will use the units MW/Hz and s^{-1}, respectively.

First, we derive the stability region of the Nth-order model in the droop coefficient space. Since we have a 6-dimensional space, we fix the inertial droop coefficients to $(h_1, h_2, h_4) = (359.8,\ 10.73,\ 400)$, and plot the stable region in a 3-dimensional frequency droop space as shown in Fig. 4. The concave region of the petal-like surface is the stable region. Next, we fix the frequency droop coefficients to $(k_{f1},\ k_{f2},\ k_{f4}) = (404.24,\ 152.43,\ 300)$ and show the boundary of the stable region in the inertial droop coefficient space, see Fig. 5.

Finally, we compare the region of stability between the Nth-order and the full-order model with $(h_1,\ h_2\ ,h_4) = (0,\ 0,\ 0)$. The stability boundary of the full-order model is obtained numerically through linearization toolbox of Matlab [31]. It can be observed that the stable region postulated by the stability theorem closely matches that of the full-order model.

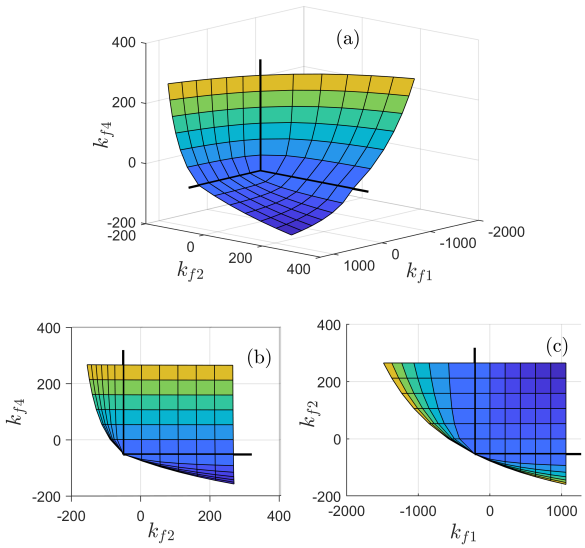

Fig. 4: Stability boundary of the Nth-order model in the frequency droop space with $(h_1,\ h_2,\ h_4) = (359.8,\ 10.73,\ 400)$: (a) The boundary as viewed from stable region, (b) top view (X-Y view) and (c) side view (X-Z view).

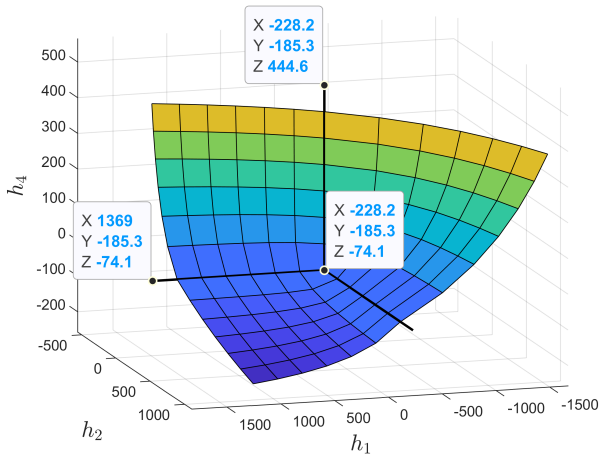

Fig. 5: Stability boundary of the Nth-order model in the inertial droop space with $(k_{f1},\ k_{f2},\ k_{f4}) = (404.24,\ 152.43,\ 300)$: The boundary as viewed from stable region.

V. Conclusion

In this paper, we proved a stability theorem that establishes the region of small-signal stability of the reduced-order model of an AC-MTDC grid in the droop coefficient space of the MTDC converter controls. The proof considers inertial and frequency droop control acting simultaneously, which was not done in the existing literature. A case study shows that the postulated stable region closely matches with that of the full-order model.

Appendix: Derivation of $\mathbf{H_N}^{-1}\mathbf{K_N}$

We consider notations used in the proofs of Lemma III.3 and Theorem III.1. We express $\mathbf{H_N}$ and $\mathbf{K_N}$ as follows

$$\mathbf{H_N} = \mathbf{A_1} + \mathbf{u}\mathbf{v_1^T}, \quad \mathbf{K_N} = \mathbf{A_2} + \mathbf{u}\mathbf{v_2^T}$$

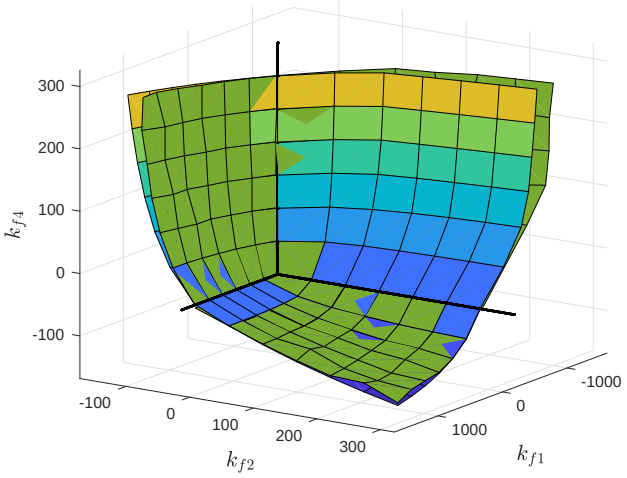

Fig. 6: Stability boundary of the Nth-order model (colormap) vs the full-order model (green) with $(h_1,\ h_2\ ,h_4) = (0,\ 0,\ 0)$.

where, $\mathbf{A_1} = diag\left([p_i]_N\right)$, $\mathbf{A_2} = diag\left([q_i]_N\right)$, $\mathbf{v_1} = [h_i]_N$, $\mathbf{v_2} = \left[k_{fi}\right]_N$, $\mathbf{u} = \left[-\bar{k}_{vi}\right]_N$.

Let us assume $g = trace\left(\mathbf{u}\mathbf{v_1^T}\mathbf{A_1^{-1}}\right)$. We note the following: $\mathbf{u^T 1} = -1$ and $g = \mathbf{v_1^T}\mathbf{A_1^{-1}}\mathbf{u} = \sum \frac{c_i}{p_i}\bar{k}_{vi} - 1 = w - 1$. Using the Sherman-Morrison formula [27], we can write

$$\begin{aligned}\mathbf{H_N^{-1}K_N} &= \left(\mathbf{A_1} + \mathbf{u}\mathbf{v_1^T}\right)^{-1}\left(\mathbf{A_2} + \mathbf{u}\mathbf{v_2^T}\right)\\ &= \left(\mathbf{A_1^{-1}} - \tfrac{1}{g+1}\mathbf{A_1^{-1}}\mathbf{u}\mathbf{v_1^T}\mathbf{A_1^{-1}}\right)\left(\mathbf{A_2} + \mathbf{u}\mathbf{v_2^T}\right)\end{aligned}$$

Upon expansion, we can write

$$\begin{aligned}&\mathbf{H_N^{-1}K_N} = \mathbf{A_1^{-1}A_2} + \mathbf{A_1^{-1}u}\left(\mathbf{v_2^T} - \tfrac{1}{g+1}\mathbf{v_1^T}\mathbf{A_1^{-1}}\left(\mathbf{A_2} + \mathbf{u}\mathbf{v_2^T}\right)\right)\\ &= \mathbf{A_1^{-1}A_2} + \mathbf{A_1^{-1}u}\left(\mathbf{v_2^T} - \tfrac{g}{g+1}\mathbf{v_2^T} - \tfrac{1}{g+1}\mathbf{v_1^T}\mathbf{A_1^{-1}A_2}\right)\\ &= \mathbf{A_3} + \tfrac{1}{1+g}\mathbf{u_1}\left(\mathbf{v_2^T} - \mathbf{v_1^T}\mathbf{A_3}\right)\end{aligned}$$

where, $\mathbf{A_3} = \mathbf{A_1^{-1}A_2}$, $\mathbf{u_1} = \mathbf{A_1^{-1}u}$.

Remark: As shown above, the matrix $\mathbf{H_N^{-1}K_N}$ can be expressed as rank-1 perturbation of a diagonal matrix $\mathbf{A_1^{-1}A_2}$ simply because $\mathbf{A_1^{-1}u}$ can be taken common from the remaining terms. *This is possible, since vector* $\mathbf{u}$ *is common in the rank-1 perturbation terms of both* $\mathbf{H_N}$ *and* $\mathbf{K_N}$. ■

It can be shown that

$$\begin{aligned}&\mathbf{u_1} = \left[-\frac{\bar{k}_{vi}}{p_i}\right]_N, \quad \mathbf{v_1^T}\mathbf{A_3} = \left[q_i - \frac{c_i q_i}{p_i}\right]_N^T\\ &\mathbf{A_3} = diag\left(\left[\frac{q_i}{p_i}\right]_N\right), \quad \mathbf{v_2^T} - \mathbf{v_1^T}\mathbf{A_3} = \left[\frac{c_i q_i}{p_i} - d_i\right]_N^T.\end{aligned}$$

This leads to

$$\mathbf{H_N^{-1}K_N} = diag\left(\left[\frac{q_i}{p_i}\right]_N\right) + \frac{1}{w}\left[\frac{\bar{k}_{vi}}{p_i}\right]_N\left[d_i - \frac{c_i q_i}{p_i}\right]_N^T.$$

References

[1] Energy Emergencies Executive Committee, *GB power system disruption - 9 august 2019*, September 2019.

[2] DESERTEC Foundation, www.desertec.org.

[3] J. Dai, Y. Phulpin, A. Sarlette, and D. Ernst, "Coordinated primary frequency control among non-synchronous systems connected by a multi-terminal high-voltage direct current grid," *IET Generation, Transmission Distribution*, vol. 6, no. 2, pp. 99–108, Feb. 2012, ISSN: 1751-8687. DOI: 10.1049/iet-gtd.2011.0312.

[4] A. Sarlette, J. Dai, Y. Phulpin, and D. Ernst, "Cooperative frequency control with a multi-terminal high-voltage DC network," *Automatica*, vol. 48, no. 12, pp. 3128–3134, 2012, ISSN: 0005-1098. DOI: https://doi.org/10.1016/j.automatica.2012.08.017.

[5] F. D. Bianchi and J. L. Domnguez-Garca, "Coordinated frequency control using MT-HVDC grids with wind power plants," *IEEE Transactions on Sustainable Energy*, vol. 7, no. 1, pp. 213–220, Jan. 2016, ISSN: 1949-3029. DOI: 10.1109/TSTE.2015.2488098.

[6] P. M. Namara, R. R. Negenborn, B. D. Schutter, G. Lightbody, and S. McLoone, "Distributed MPC for frequency regulation in multi-terminal HVDC grids," *Control Engineering Practice*, vol. 46, pp. 176–187, 2016, ISSN: 0967-0661. DOI: https://doi.org/10.1016/j.conengprac.2015.11.001.

[7] M. Andreasson, R. Wiget, D. V. Dimarogonas, K. H. Johansson, and G. Andersson, "Coordinated frequency control through MTDC transmission systems," *IFAC-PapersOnLine*, vol. 48, no. 22, pp. 106–111, 2015, ISSN: 2405-8963. DOI: http://dx.doi.org/10.1016/j.ifacol.2015.10.315.

[8] M. Andreasson, R. Wiget, D. V. Dimarogonas, K. H. Johansson, and G. Andersson, "Distributed frequency control through MTDC transmission systems," *IEEE Transactions on Power Systems*, vol. 32, no. 1, pp. 250–260, Jan. 2017, ISSN: 0885-8950. DOI: 10.1109/TPWRS.2016.2555939.

[9] P. McNamara and F. Milano, "Model predictive control based AGC for multi-terminal HVDC-connected AC grids," *IEEE Transactions on Power Systems*, vol. PP, no. 99, pp. 1–1, 2017, ISSN: 0885-8950. DOI: 10.1109/TPWRS.2017.2694768.

[10] T. M. Haileselassie and K. Uhlen, "Primary frequency control of remote grids connected by multi-terminal HVDC," in *IEEE PES General Meeting*, Jul. 2010, pp. 1–6. DOI: 10.1109/PES.2010.5589327.

[11] B. Silva, C. L. Moreira, L. Seca, Y. Phulpin, and J. A. P. Lopes, "Provision of inertial and primary frequency control services using offshore multiterminal HVDC networks," *IEEE Transactions on Sustainable Energy*, vol. 3, no. 4, pp. 800–808, Oct. 2012, ISSN: 1949-3029. DOI: 10.1109/TSTE.2012.2199774.

[12] I. M. Sanz, B. Chaudhuri, and G. Strbac, "Inertial response from offshore wind farms connected through DC grids," *IEEE Transactions on Power Systems*, vol. 30, no. 3, pp. 1518–1527, May 2015, ISSN: 0885-8950. DOI: 10.1109/TPWRS.2014.2349739.

[13] Y. Li and Z. Xu, "Coordinated control of wind farms and MTDC grids for system frequency support," *Electric Power Components and Systems*, vol. 45, no. 4, pp. 451–464, 2017. DOI: 10.1080/15325008.2016.1264500.

[14] I. M. Sanz, B. Chaudhuri, and G. Strbac, "Frequency changes in AC systems connected to DC grids: Impact of AC vs. DC side events," in *2014 IEEE PES General Meeting — Conference Exposition*, Jul. 2014, pp. 1–5. DOI: 10.1109/PESGM.2014.6939914.

[15] S. Akkari, J. Dai, M. Petit, and X. Guillaud, "Coupling between the frequency droop and the voltage droop of an AC/DC converter in an MTDC system," in *2015 IEEE Eindhoven PowerTech*, Jun. 2015, pp. 1–6. DOI: 10.1109/PTC.2015.7232285.

[16] L. Papangelis, X. Guillaud, and T. V. Cutsem, "Frequency support among asynchronous AC systems through VSCs emulating power plants," in *11th IET International Conference on AC and DC Power Transmission*, Feb. 2015, pp. 1–9. DOI: 10.1049/cp.2015.0033.

[17] L. Papangelis, M.-S. Debry, P. Panciatici, and T. V. Cutsem, "A receding horizon approach to incorporate frequency support into the AC/DC converters of a multi-terminal DC grid," *Electric Power Systems Research*, vol. 148, pp. 1–9, 2017, ISSN: 0378-7796. DOI: https://doi.org/10.1016/j.epsr.2017.03.007.

[18] L. Papangelis, M. S. Debry, T. V. Cutsem, and P. Panciatici, "Local control of AC/DC converters for frequency support between asynchronous AC areas," in *2017 IEEE Manchester PowerTech*, Jun. 2017, pp. 1–6. DOI: 10.1109/PTC.2017.7980876.

[19] L. Papangelis, M.-S. Debry, T. Prevost, P. Panciatici, and T. V. Cutsem, "Decentralized model predictive control of voltage source converters for AC frequency containment," *International Journal of Electrical Power & Energy Systems*, vol. 98, pp. 342–349, 2018, ISSN: 0142-0615. DOI: https://doi.org/10.1016/j.ijepes.2017.12.015.

[20] R. Wang, L. Chen, T. Zheng, and S. Mei, "VSG-based adaptive droop control for frequency and active power regulation in the MTDC system," *CSEE Journal of Power and Energy Systems*, vol. 3, no. 3, pp. 260–268, Sep. 2017. DOI: 10.17775/CSEEJPES.2017.00040.

[21] W. Wang, Y. Li, Y. Cao, U. Haeger, and C. Rehtanz, "Adaptive droop control of MTDC system for frequency support and power sharing," *IEEE Transactions on Power Systems*, vol. PP, no. 99, pp. 1–1, 2017, ISSN: 0885-8950. DOI: 10.1109/TPWRS.2017.2719002.

[22] S. G. Vennelaganti and N. R. Chaudhuri, "Selective power routing in MTDC grids for inertial and primary frequency support," *IEEE Transactions on Power Systems*, vol. 33, no. 6, pp. 7020–7030, Nov. 2018, ISSN: 0885-8950. DOI: 10.1109/TPWRS.2018.2854647.

[23] ——, "Ratio-based selective inertial and primary frequency support through MTDC grids with offshore wind farms," *IEEE Transactions on Power Systems*, vol. 33, no. 6, pp. 7277–7287, Nov. 2018, ISSN: 0885-8950. DOI: 10.1109/TPWRS.2018.2850145.

[24] A. Kirakosyan, E. F. El-Saadany, M. S. El Moursi, and M. Salama, "Selective frequency support approach for MTDC systems integrating wind generation," *IEEE Transactions on Power Systems*, in early access, 2020.

[25] S. G. Vennelaganti and N. R. Chaudhuri, "Stability criterion for inertial and primary frequency droop control in MTDC grids with implications on ratio-based frequency support," *IEEE Transactions on Power Systems*, vol. 35, no. 5, pp. 3541–3551, 2020.

[26] B. Berggren, K. Lindén, and R. Majumder, "Dc grid control through the pilot voltage droop concept—methodology for establishing droop constants," *IEEE Transactions on Power Systems*, vol. 30, no. 5, pp. 2312–2320, 2015. DOI: 10.1109/TPWRS.2014.2360585.

[27] M. S. Bartlett, "An inverse matrix adjustment arising in discriminant analysis," *Ann. Math. Statist.*, vol. 22, no. 1, pp. 107–111, Mar. 1951. DOI: 10.1214/aoms/1177729698. [Online]. Available: https://doi.org/10.1214/aoms/1177729698.

[28] M. Zedek, "Continuity and location of zeros of linear combinations of polynomials," *Proc. Amer. Math. Soc.*, 16 (1965), 78-84. DOI: 10.1090/S0002-9939-1965-0171902-8.

[29] B. Barmish, *New Tools for Robustness of Linear Systems*, ser. Irwin Series in Finance. Prentice Hall PTR, 1994, ISBN: 9780023060557. [Online]. Available: https://books.google.co.in/books?id=vP5QAAAAMAAJ.

[30] N. R. Chaudhuri, B. Chaudhuri, R. Majumder, and A. Yazdani, *Multi-terminal Direct Current Grids : Modeling, Analysis, and Control*. Oxford: Wiley/IEEE Press, 2014.

[31] *MATLAB version 9.8.0.1396136 (R2020a)*, The Mathworks, Inc., Natick, Massachusetts, 2020.